Segregation of motor and sensory axons regenerating through bicompartmental tubes by combining extracellular matrix components with neurotrophic factors

Jaume del Valle [1,2,3,*], Daniel Santos [1,2,*], Ignacio Delgado-Martínez [1], Natàlia de la Oliva[1], Guido Giudetti [4], Silvestro Micera [4,5], Xavier Navarro [1,2]

[1] Institute of Neurosciences and Department of Cell Biology, Physiology and Immunology, Universitat Autònoma de Barcelona

[2] Centro de Investigación Biomédica en Red sobre Enfermedades Neurodegenerativas (CIBERNED), Bellaterra, Spain

[3] Catalan Institute of Nanoscience and Nanotechnology (ICN2), CSIC and BIST, Bellaterra, Spain

[4] The BioRobotics Institute, Scuola Superiore Sant'Anna, Pontedera, Italy

[5] Translational Neural Engineering Laboratory, Center for Neuroprosthetics and Institute of Bioengineering, École Polytechnique Fédérale de Lausanne (EPFL), Lausanne, Switzerland

* Both authors contributed equally to this study

Running title: Motor and sensory axon regeneration by combining ECM and NTFs

Keywords: Y-tube, neurotrophic factors, extracellular matrix, motor axons, sensory axons, axonal guidance, axon regeneration.

Corresponding author: Dr. Xavier Navarro. xavier.navarro@uab.cat

Abstract

Segregation of regenerating motor and sensory axons may be a good strategy to improve selective functionality of regenerative interfaces to provide close loop commands. Provided that extracellular matrix (ECM) components and neurotrophic factors (NTFs) exert guidance effects on different neuronal populations, we assessed in vivo the potential of separating sensory and motor axons regenerating in a bicompartmental Y-type tube, with each branch prefilled with an adequate combination of ECM and NTFs.

The severed rat sciatic nerve was repaired using a bicompartmental tube filled with a collagen matrix enriched with fibronectin and BDNF encapsulated in PLGA microspheres (FN+MP.BDNF) in one compartment to preferentially attract motor axons and collagen enriched with laminin and NGF and NT-3 in microspheres (LM+MP.NGF/NT-3) in the other compartment for promoting sensory axons regeneration. Control animals were implanted with the same Y-tube with a collagen matrix with microspheres containing PBS (Col+MP.PBS).

By using retrotracer labeling, we found that LM+MP.NGF/NT-3 did not attract higher number of regenerated sensory axons compared to controls, and no differences were observed in sensory functional recovery. However, FN+MP.BDNF guided a higher number of regenerating motor axons compared to controls, improving also motor recovery. A small proportion of sensory axons with large soma size, likely proprioceptive neurons, was also attracted to the FN+MP.BDNF compartment. These results demonstrate that muscular axonal guidance can be modulated in vivo by the addition of fibronectin and BDNF.

1. Introduction

Neuroprosthetic devices have been evolving in the last years in order to replace and restore limb functionality to amputee patients. Advanced neuroprostheses offer a high number of degrees of freedom and sensors (Carrozza et al., 2006); however, these robotic innovations are not matched by a suitable neural interface technology. Thus, there is still need for closed loop commands for precise execution of movements and incorporating input to the sensory neurons, i.e. the integration of both sensory neuron (SN) and motor neuron (MN) functions on the interface device. Therefore, the topographical separation of regenerating axons from sensory and motor neurons in mixed nerves could be a good approach to selectively stimulate or record different neural signals by means of regenerative interfaces to obtain improved neuroprosthetic control (Delgado-Martinez et al., 2017).

Previous studies described the existence of a preferential motor reinnervation (PMR), in which regenerating motor axons tend to enter into distal muscle branches in higher proportion than into cutaneous branches (Brushart, 1988). Similarly, the muscle branch was also more prone to be reinnervated by muscular than by cutaneous sensory afferents (Madison et al., 1996). This phenomenon of preferential reinnervation has been attributed to the specific interactions between regenerating axons and the environment generated in the denervated distal nerve branches (Brushart et al., 1998). Several studies have focused in elucidating different contributors for the PMR effect. Schwann cells have been suggested to have a specific identity that can be recognized by regenerating axons due to differential motor or sensory phenotypes and expression of particular surface receptors. Thus, the HNK-1 carbohydrate epitope is expressed strongly in Schwann cells of motor axons in the adult rodent, but rarely in those associated to sensory axons, whereas NCAM is present exclusively in sensory nerve fascicles and not in motor fascicles (Martini et al., 1994, 1992; Saito et al., 2005). However, Schwann cells de-differentiate during Wallerian degeneration and tend to lose that preferential marker expression within days after nerve transection in motor and sensory fascicles (Lago et al., 2007; Saito et al., 2005). Another point of view suggests that it is the relative level and type of trophic support provided by each nerve branch and the target organ that determine whether motor or sensory axons regrow in that particular branch (Madison et al., 2007). Interestingly, Hoke and colleagues (Höke et al., 2006) demonstrated that Schwann cells of sensory and motor nerves produce different growth factors at baseline and respond differently during denervation and when reinnervated by cutaneous or motor axons. Thus, we hypothesized that the local sustained application of specific guidance and trophic factors might result in higher probability of directed regeneration of motor or sensory axons than grafting different populations of Schwann cells, that lost their distinct phenotype after denervation and thus have a limited effect (Höke et al., 2006; Lago et al., 2007).

Importantly, nerve growth factor (NGF) and neurotrophin-3 (NT-3) have predominant attractive properties, mediated by their TrkA and TrkC receptors, for SN both in vitro and in vivo (Bloch et al., 2001; Gallo et al., 1997; Lotfi et al., 2011; Moore et al., 2006), whereas BDNF promotes MN outgrowth in vitro (Allodi et al., 2011) and has attractive properties mediated by TrkB receptors for regenerating MNs (Henle et al., 2011; Li et al., 2005; Song et al., 1997; Yuan et al., 2003). In addition, different extracellular matrix (ECM) components constituents of the endoneurial tubes and the basal lamina play a role in the promotion of preferential axon outgrowth. For instance, laminin substrate mainly promotes sensory axon outgrowth in vitro (Gardiner, 2011; Plantman et al., 2008), whereas fibronectin enhances motor and proprioceptive axon outgrowth (González-Pérez et al., 2016). Therefore, the addition of different combination of neurotrophic factors and ECM components in a Y tube model could be an interesting approach for segregating motor and sensory axons. In fact, a previous study used a Y-tube model to separate regenerating TrkC-expressing proprioceptive from TrkA-expressing nociceptive neurons by the addition of NT-3 and NGF, respectively (Lotfi et al., 2011).

In the present study, a sciatic nerve transection was repaired with a bicompartmental tube containing a different combination of ECM and neurotrophic factors in each distal branch. Based on our previous results (Santos et al., 2017a, 2016a, 2016b), each compartment was filled prior to implantation with a collagen matrix containing either fibronectin with PLGA microspheres releasing BDNF (FN+MP.BDNF) in one side in contact with the distal peroneal nerve (P), or laminin with PLGA microspheres releasing NGF and NT-3 (LM+MP.NGF/NT-3) at the other side in contact with the tibial and sural nerves (T+S). We assessed whether regenerated motor axons preferentially grew in the first branch and sensory axons in the second branch, compared to control condition in which both branches contained the same collagen matrix and PLGA microspheres filled with PBS (Col+MP.PBS).

2. Materials and methods

2.1. Ethics statement

The experimental procedures were approved by the ethical committee of the Universitat Autonoma de Barcelona in accordance with the European Communities Council Directive 2010/63/EU. Female Sprague-Dawley rats (250–300 g) were used for the *in vivo* studies. They were kept on standard laboratory conditions with a light-dark cycle of 12:12 h and *ad libitum* access to food and tap water. All efforts were made to minimize pain and animal discomfort during surgery and treatments.

2.2. Fabrication of the bicompartmental tube and implantation

The Y-tube consisted of a silicone tube divided in two sections by a flat polyimide film. Silicone tubes (8 mm long, 2 mm i.d.) were cut longitudinally along 4 mm and a polyimide film (8 mm long, 2 mm wide, 30 µm thick) was placed along the midline to divide the distal half tube into two separated chambers. To prevent distal axon reorganization, 4 mm of the polyimide film extended out of the tube (see Fig. 1A, B). The slit cut of the tube was closed with silicone adhesive to hold the film in place.

NGF, NT-3, and BDNF were encapsulated in Poly-lactic Co-Glycolic acid microspheres (MPs) as previously described (Giudetti et al., 2014). MPs containing NGF and NT-3 were added to a collagen type I solution (3 mg/ml; #354236, Corning) supplemented with laminin 20% (Sigma) to reach a final concentration of 1 µg/ml for each trophic factor. Similarly, BDNF containing MPs were added to a collagen solution supplemented with fibronectin 20% (BD Biosciences) to reach a final concentration of 2 µg/ml for BDNF. In the experimental group, each branch of the Y-tube was filled with one of the above solutions (Fig. 1B). In the control group, both branches were filled with collagen gel mixed with MPs containing PBS (Col+MP.PBS) (Fig. 1A). Tubes were maintained vertically for 12 hours before surgery in order to promote fibril alignment during gel formation (Verdú et al., 2002).

Animals were anaesthetized with ketamine/xylacine (90/10 mg/kg i.p.), the sciatic nerve was exposed at the midthigh, transected and a portion of 3 mm resected. The proximal sciatic nerve stump was sutured to the proximal end of the bicompartmental tube. The distal stump was carefully dissected to separate the P, T and S nerve branches; then, the distal P nerve was inserted in the compartment containing FN+MP.BDNF, whereas the T+S nerves were inserted in the compartment containing LM+MP.NGF/NT-3 (Fig. 1C). The nerve stumps were fixed with one 10-0 suture stitch, leaving an interstump distance of 6 mm. The wound was closed by planes with silk sutures. Animals were kept for 90 days to allow axonal regeneration.

2.3. Assessment of skin sensory reinnervation.

The progression of nociceptive reinnervation of the hindpaw was assessed by means of the pinprick test and thermal algesimetry at 7, 30, 45, 60, 75 and 90 days postinjury (dpi). For the pinprick test, animals were gently kept in a cloth with the sole of the injured paw facing upward, and the skin was stimulated with a needle from proximal to distal at specific sites of the lateral side of the plantar surface (Cobianchi et al., 2014). Positive withdrawal responses were taken as sign of skin functional reinnervation and recorded only when clear pain reaction was triggered by the stimulation. A composite score was calculated as the mean number of responses per group at each day of testing.

Thermal sensitivity was assessed using a Plantar test algesimeter (Ugo Basile, Comerio, Italy). Rats were placed into a plastic box with an elevated plexiglass floor. The beam of a lamp was pointed to the lateral part in the hindpaw plantar surface. Intensity was set to low power (40 mW/cm^2) with a heating rate of 1°C/s to elicit activation of unmyelinated fibers as described before (Cobianchi et al., 2014). A cutoff time for the stimuli was set at 20 seconds to prevent tissue damage. Heat pain threshold was calculated as the mean of 3 trials per test site, with a 5-minute resting period between each trial, and expressed as the latency (in seconds) of paw withdrawal response.

2.4. Assessment of motor reinnervation

Functional reinnervation of target muscles was assessed at 90 dpi before the retrotracer application. Briefly, animals were anesthetized with ketamine/xylacine and sub-dermal steel needle electrodes were placed transcutaneously at the sciatic notch for electrical stimulation using single monophasic pulses of 100 µs duration (Synergy Medelec, Viasys HealthCare). The compound muscle action potentials (CMAPs) of tibialis anterior (TA), gastrocnemius medialis (GM) and plantar interossei (PL) muscles were recorded using steel needles in monopolar configuration (Santos et al., 2017b). The amplitude and latency of the M-wave were measured and the contralateral intact limb was used as control. The rat body temperature was maintained by means of a thermostated warming flat coil throughout the test.

2.5. Retrograde labeling and neuronal counting

To quantify motor and sensory regenerated neurons, rats were anaesthetized with ketamine/xylacine, the sciatic nerve was carefully dissected and the silicone tube removed. The regenerated nerve branches were transected at the distal part, separated from the polyimde wall, and dipped in 5 µl of Fluorogold (FG; 5%; Fluorochrome Inc.) or True Blue (TB; 5%; Setareh Biotech) for 1 hr inside a vaseline well. Retrotracer application was counterbalanced in order to minimize possible differences between retrotracers efficacy (Zele et al., 2010). After retrieval of the well, the area was rinsed with saline to clean any remnants of the tracer and the wound sutured. Animals were allowed to survive for 7 days for

accumulation of the tracer in the soma of spinal motoneurons and DRG sensory neurons. Then, rats were deeply anesthetized and transcardially perfused with 4% paraformaldehyde in PBS. The lumbar segment (L3-L6) of the spinal cord and the L4 and L5 DRG were removed, postfixed at 4ºC in the same fixative solution for 1h and transferred to 30% sucrose in PBS. The cord and DRG were cut in a cryostat longitudinally in 40 and 20 µm thick sections respectively, mounted on slides, heated at 35ºC for 1h and stored at -20ºC in the dark. Finally, sections were observed with an Olympus BX51 fluorescence microscope under UV light and the number of FG, TB and double labelled (DL) neurons were counted in every third section following the fractionator principle (Gundersen, 1986).

2.6. Morphometric analysis

The identification of labelled SNs was done using Fiji software (Schindelin et al., 2013). RGB pictures were converted to L*a*b* colour space to extract the 'a*' channel, containing the information of the tracer fluorescence. The resulting image was smoothed using a median filter. A binary image was generated using a mid-grey adaptive local thresholding procedure. Soma clusters were extrapolated using a watershed algorithm. Neuron-like objects were then identified by the "Analyze particles" tool of the software and manually verified. The data about number of objects and their area and 'a*' value were further analysed in SPSS 22.0 (IBM Corp., USA). Objects were clustered using a k-means procedure according to two independent features, area and mean value of the 'a*' channel. From the area, three groups were selected: small (<600 μm^2), medium (600-1200 μm^2) and large size (>1200 μm^2), according to previously defined size criteria (Fukuoka et al., 2001). From the value of the 'a*' channel, objects were separated into TB^+, FG^+, DL^+. TB^+ and FG^+ objects were assigned to the corresponding reinnervating branch based on the experimental settings.

2.7. Data analysis

Data are presented as mean ± SEM. Results were statistically analyzed by using GraphPad Prism (GraphPad Software, USA). Student t-test and one and two-way ANOVA followed by Bonferroni's post hoc tests for comparison between groups were used. Statistical significance was considered when P value was <0.05.

3. Results

3.1 Sensory and motor functional recovery

Sensory functional recovery, evaluated by mechanical and thermal tests, did not show differences between control and experimental groups. For pinprick test, the first responses were observed at 30 dpi, without significant differences between groups at any time points (Fig. 2A). Similarly, withdrawal responses in the plantar test reappeared at 30 dpi and no differences were observed during the follow-up between groups (Fig. 2B). These results indicate that the branch containing LM+MP.NGF/NT-3 did not promote higher regeneration of SNs to the T+S nerves in comparison with the control condition.

Electrophysiological tests were performed to assess reinnervation of the TA, GM and PL muscles (Fig. 3). The amplitude of the TA CMAP (Fig. 3A) was higher in FN+MP.BDNF than in the control group (27.5 ± 2.9 mV and 22.3 ± 2.7 mV, respectively, $p<0.05$) suggesting that a higher number of MNs had regenerated towards the chamber which contained FN+MP.BDNF and was sutured to the P nerve that innervates the TA muscle. In contrast, the GM and PL CMAPs (Fig. 3 B, C) were higher in the control than in the LM+MP.NGF/NT-3 condition ($p<0.05$ for the GM CMAP) indicating that a lower number of MNs had regenerated towards the T+S nerves with LM+MP.NGF/NT-3 in comparison with the control condition.

3.2 Motor and sensory neuron directed regeneration

At the final time point, we observed that all the animals had a regenerated nerve within the Y-tube that bifurcated in each compartment created by the polyimide film to distally reinnervate the P nerve at one side and T+S nerves at the other side (Fig. 1D).

Retrotracer application confirmed that in all the rats MNs and SNs had regenerated through the Y tube, as judged by the presence of TB+, FG+ and DL neurons (Fig. 4A-C) in SC and DRG sections (Fig. 4D-G). Data on the total number of retrolabeled neurons for each condition are shown in Table 1. The number of regenerated neurons was about 8500 in both groups, but there were differences between branches and distribution. Thus, in the experimental group about 1200 more neurons regenerated their axons in the branch towards the P nerve and correspondingly less towards the T+S nerves than in the control group.

When counting the number of retrolabeled MNs, in the control group 74.1±1.2% of the MNs regenerated towards the T+S distal stump, whereas only 10.0±4.1% regenerated towards the P nerve. In addition, 15.8±6.4% MNs were DL suggesting the formation of axonal sprouts that grew through both branches of the tube. On the other hand, in the experimental group 53.5±6.5% of regenerated MNs grew towards the FN+MP.BDNF branch connected to the P nerve ($p<0.001$ vs the control condition, Fig. 4H). Consequently, less MNs regenerated through

the LM+MP.NGF/NT-3 compartment (36.6±6.5%; p<0.001 vs the control condition). There were no differences in the number of DL MNs between the two groups.

Regarding retrolabeled SNs, in the control group 67.0±4.4% grew towards the T+S distal stump and only 23.9±9.0% towards the P distal nerve, whereas 9.0±1.5% were DL neurons. The addition of different combination of ECM and NTFs into separate branches of the Y tube had a slight but not significant influence on regeneration of sensory axons, since 56.8±14% were labeled from the LM+MP.NGF/NT-3 branch, 34.7±9.3% from the FN+MP.BDNF branch and 8.43±2.2 from both chambers (Fig. 4I).

These results demonstrate that the addition of LM+MP.NGF/NT-3 did not exert a significant effect attracting regenerating SNs, whereas the addition of FN+MP.BDNF significantly attracted more regenerating MNs compared to the control condition.

3.3. FN+BDNF preferentially attract large sensory neurons

Since SNs are constituted by a heterogeneous population (Usoskin et al., 2015), we performed a morphometric analysis to characterize differences in size of SNs that regenerated at different branches of the bicompartmental tube.

The frequency distribution of regenerated SNs showed no differences in soma size of sensory neurons that regenerated in the LM+MP.NGF/NT-3 branch compared to the control gel (Fig. 5A). However, SNs that regenerated in the FN+MP.BDNF gel towards the P nerve showed a larger soma size profile than in the control gel. Then, we grouped the regenerated SNs in small, medium and large size to further characterize the composition of each regenerating branch (Fig. 5D-F). The only significant difference in size was observed between FN+MP.BDNF and Col+MP.PBS conditions for large SNs (p<0.05, Fig. 5F). These results demonstrate that the combination of FN and BDNF promoted the directed growth of large sensory axons, which are related with muscular afferents (Taylor et al., 2005).

4. Discussion

In this study we have used a bicompartmental tube model that forces the regenerating axons to grow along a different branch. When the axons regenerate within the tube, they may choose between two branches with a different milieu to grow. By manipulating the composition of the inside matrix of each branch we attempted to preferentially attract the regenerating motor and sensory axons and then selectively guide them towards different distal nerves and their corresponding targets. In accordance with similar studies with gap defects (Clements et al., 2009; Meyer et al., 2016; Santos et al., 2016b), the division of the tube in two separated compartments did not suppose an obstacle for nerve regeneration as all the operated animals showed regeneration distal to the tube and evidence of functional reinnervation of skin and

muscles. Tube repair leaving a short gap between proximal and distal nerve stumps was first presumed to allow axons to be guided towards their original distal fascicle by means of neurotropic diffusible factors (Evans et al., 1991; Rende et al., 1991). However, later studies proved that tube repair by itself did not improve the selectivity of regeneration with respect to direct suture when correct alignment between proximal and distal stumps was achieved (Bodine-Fowler et al., 1997; Valero-Cabré et al., 2001, 2004).

Therefore, we have evaluated here if the addition of a different combination of ECM molecules and NTFs into a collagen matrix was able to selectively promote the regeneration of motor and sensory neurons towards different distal fascicles. We chose the two matrix combinations based on previous in vitro findings using organotypic cultures that demonstrated a preferential effect of fibronectin and BDNF to promote neurite growth from MNs and of laminin and NGF/NT-3 to promote neurite growth of SNs (González-Pérez et al., 2016; Santos et al., 2017a). The distal insert was selected to accommodate the size of the distal nerve with the number of axons of each type. Since there are many more sensory than motor axons in the sciatic nerve, the largest distal nerve (tibial+sural) was placed in the compartment for preferential growth of sensory axons, whereas the smaller peroneal nerve was placed in the compartment for motor axons.

Retrotracer labeling quantification of regenerated motor and sensory neurons when placing the control collagen matrix in the tube branches showed no significant differences between branches connected distally with the T+S nerves and the P nerve. Moreover, about 15% of motor and 9% of sensory neurons generated regenerative sprouts that grew towards both branches. Due to the fact that T, S and P are mixed nerves, no preferential influence on motor or sensory neuron regeneration was expected (Brushart, 1993; Brushart et al., 1998). The higher percentage of motor and sensory neurons regenerating to the T+S branch than to the P branch can be attributed to the larger caliber of the former that contains larger number of Schwann cells that generate higher concentration of trophic and tropic factors in the distal nerve (Abernethy et al., 1992; Robinson and Madison, 2004; Takahashi et al., 1999; Uschold et al., 2007).

On the other hand, in the experimental group we found that adding FN+MP.BDNF at one branch of the tube and LM+MP.NGF/NT-3 to the other branch resulted in higher number of MNs that regenerated their axons towards the first condition compared to the control group. In accordance, higher CMAP amplitudes were recorded in TA muscles of animals treated with FN+MP.BDNF and lower CMAPS for the LM+MP.NGF/NT-3 indicating that more motor fibers had reinnervated the muscles provided by the P nerve than those by the T nerve. The addition of FN+MP.BDNF to the branch in contact with the P nerve was able to partially overcome the size attracting effect of the T+S nerves and attracted more than 50% of motor axons. In fact, BDNF is a potent neurotrophic factor for MNs regeneration (Allodi et al., 2011; Boyd and

Gordon, 2002; Vögelin et al., 2006), and it has been reported that the same intracellular mechanisms that promote axonal growth and cell survival are related with axonal guidance (Henle et al., 2011; Ming et al., 1999; Yuan et al., 2003). Furthermore, fibronectin also preferentially promotes motor axon outgrowth in vitro (González-Pérez et al., 2016). In addition, it is possible that FN or BDNF act not only directly on the regenerating fibers but also they may promote the recruitment of motor-related Schwann cells (Jesuraj et al., 2012). The enhancing effect shown is of relevance given the reduced regeneration of motor fibers compared to sensory fibers in tube repair of mid to long gaps (Madorsky et al., 1998; Navarro et al., 1994).

Contrary to our hypothesis, addition of laminin and NGF/NT-3 was not able to promote attraction of sensory axons, and in fact, a non-significantly lower proportion of regenerating SNs was labeled from the TS branch than with the control collagen gel. This result was corroborated by lack of differences in sensory functional recovery between both control and experimental groups. The lack of effect of LM+MP.NGF/NT-3 on SNs was not expected as previous studies described a trophic and tropic guidance effect for laminin and NGF and NT-3 individually assessed (Gallo et al., 1997; Santos et al., 2016a, 2016b; Turney and Bridgman, 2005; Webber et al., 2008). One possible reason could be related with the heterogeneous populations of SNs (Usoskin et al., 2015) that reside in the DRG, in which approximately 70% of neurons express Trk receptors but of different subtypes whereas 30% are non-peptidergic neurons and respond to GDNF (Tucker and Mearow, 2008). Laminin substrate did not show effects on non-peptidergic neurons as they express α7 integrin receptor at low levels (Gardiner et al., 2005); but there are no studies assessing fibronectin for guidance of non-peptidergic axons. In addition, among the Trk+ SNs, a low percentage of neurons express only one type of Trk receptor (23%), whereas coexpression of different Trk receptors is more abundant (47%) (Karchewski et al., 1999). Then, the attracting effect mediated by the addition of LM+NGF/NT-3 could be masked by the heterogeneity of the DRG neuronal populations, which may be non-responding to NGF and NT-3 or responding to BDNF, so that sorting sensory axons is a complex task. Moreover, it has been reported that mRNA for NGF and also for BDNF, among others, were expressed vigorously by denervated cutaneous nerves (Höke et al., 2006). Therefore, it may be well considered that the increased supply of both factors one at each branch of the Y tube did not allow for an effective preferential guidance for sensory axons.

A first analysis of the differential growth of sensory axons was attempted by subdividing the regenerated SNs by soma size. Indeed, we observed a slight increase of medium and large SNs towards the FN+BDNF branch. It should be taken into account that proprioceptive neurons, characterized by their large size diameter (Taylor et al., 2005; Tucker and Mearow, 2008), respond to NT-3 (Lotfi et al., 2011) but also preferentially extend neurites on fibronectin containing substrates (González-Pérez et al., 2016). Taking into account that the

FN+MP.BDNF branch attracted a high number of motor axons, it is plausible to think that such combination promotes also regeneration of large sensory neurons that are directed towards muscular targets. Indeed, during early development, muscle sensory axons grow slightly later and become adjacent to motor axons elongating along the muscular nerve to innervate the same muscle, reflecting specific attractions between them mediated by changes in expression of cell adhesion molecules. In contrast, developing cutaneous sensory axons bundle together, and project along individual cutaneous nerves (Honig et al., 1998).

In conclusion, we demonstrate here that nerve regeneration is successful in a bicompartmental tube, in which the two branches contain a matrix with different components. We found that motor axons regeneration was promoted preferentially in the branch containing fibronectin and BDNF. The same branch also attracted axons from large SNs that might correspond to proprioceptive neurons. On the other hand, the addition of laminin and NGF/NT-3 in the other branch did not promote the growth of sensory axons. Further studies are justified to enhance the effects obtained to segregate different functional populations of axons that may be of benefit for an advanced regenerative interface.

5. Acknowledgments

This research was supported by European Union FP7-NMP project MERIDIAN under contract number 280778, and FP7-ICT project NEBIAS under contract number 611687, TERCEL (RD12/0019/0011) and CIBERNED (CB06/05/1105) funds from the Instituto de Salud Carlos III of Spain, and FEDER funds. ICN2 is supported by the Severo Ochoa program from Spanish MINECO (Grant No. SEV-2013-0295) and is Funded by the CERCA Programme / Generalitat de Catalunya. The authors thank the technical help of Monica Espejo, Marta Morell and Jessica Jaramillo.

Conflict of interests

The authors declare no financial or personal relationships between themselves and others that might bias their work. Hence, the authors declare no conflict of interest regarding the publication of this article.

6. References

Abernethy DA, Rud A, Thomas PK. 1992, Neurotropic influence of the distal stump of transected peripheral nerve on axonal regeneration: absence of topographic specificity in adult nerve. *J Anat,* **180:**395–400

Allodi I, Guzmán-Lenis MS, Hernàndez J, Navarro X, Udina E. 2011, In vitro comparison of motor and sensory neuron outgrowth in a 3D collagen matrix. *J Neurosci Methods*, **198**: 53–61

Bloch J, Fine EG, Bouche N, Zurn D, Aebischer P. 2001, Nerve growth factor- and neurotrophin-3-releasing guidance channels promote regeneration of the transected rat dorsal root. *Exp Neurol*, **172**:425–32

Bodine-Fowler S, Meyer R, Moskovitz A, Abrams R, Botte M. 1997, Inaccurate projection of rat soleus motoneurons: a comparison of nerve repair techniques. *Muscle Nerve* **20**:29–37

Boyd J, Gordon T. 2002, A dose-dependent facilitation and inhibition of peripheral nerve regeneration by brain-derived neurotrophic factor. *Eur J Neurosci*, **15**: 613–626

Brushart TM. 1993, Motor axons preferentially reinnervate motor pathways. J Neurosci, **13**: 2730–2738

Brushart TM. 1988, Preferential Axons Reinnervation of Motor Nerves by Regenerating Motor Axons. . J Neurosci, **8**: 1026–31

Brushart TM, Gerber J, Kessens P, Chen Y, Royall RM. 1998, Contributions of Pathway and Neuron to Preferential Motor Reinnervation. *J Neurosci*, **18**:8674-81

Carrozza MC, Cappiello G, Micera S, Edin B, Beccai L, Cipriani C. 2006, Design of a cybernetic hand for perception and action. *Biol Cybern*, **95**: 629–644

Clements IP, Kim Y, English AW, Lu X, Chung A, Bellamkonda R. 2009, Thin-film enhanced nerve guidance channels for peripheral nerve repair. *Biomaterials*, **30**:3834–46

Cobianchi S, de Cruz J, Navarro X. 2014, Assessment of sensory thresholds and nociceptive fiber growth after sciatic nerve injury reveals the differential contribution of collateral reinnervation and nerve regeneration to neuropathic pain. *Exp Neurol*, **255**:1–11

Delgado-Martinez I, Righi M, Santos D, Cutrone A, Bossi S, D'Amico S, Del Valle J, Micera S, Navarro X. 2017, Fascicular nerve stimulation and recording using a novel double-aisle regenerative electrode. *J. Neural Eng*, **14**:46003

Evans PJ, Bain JR, Mackinnon SE, Makino AP, Hunter DA. 1991, Selective reinnervation: a comparison of recovery following microsuture and conduit nerve repair. *Brain Res*, **559**:315–321

Fukuoka T, Kondo E, Dai Y, Hashimoto N, Noguchi K. 2001, Brain-derived neurotrophic factor increases in the uninjured dorsal root ganglion neurons in selective spinal nerve ligation model. *J Neurosci*, **21**:4891–4900

Gallo G, Lefcort FB, Letourneau PC. 1997, The trkA receptor mediates growth cone turning toward a localized source of nerve growth factor. *J Neurosci*, **17**:5445–5454

Gardiner NJ. 2011, Integrins and the extracellular matrix: key mediators of development and regeneration of the sensory nervous system. *Dev Neurobiol*, **71**:1054–72.

Gardiner NJ, Fernyhough P, Tomlinson DR, Mayer U, von der Mark H, Streuli CH. 2005, Alpha7 integrin mediates neurite outgrowth of distinct populations of adult sensory neurons, *Mol Cell Neurosci*, **28**:229–40

Giudetti G, del Valle J, Navarro X, Micera S. 2014, NGF-loaded PLGA microparticles for advanced multifunctional regenerative electrodes, *Conf Proc IEEE Eng Med Biol Soc*, **2014**:1993-5

González-Pérez F, Alé A, Santos D, Barwig C, Freier T, Navarro X, Udina E. 2016, Substratum preferences of motor and sensory neurons in postnatal and adult rats, *Eur J Neurosci*, **43**:431–442

Gundersen HJ. 1986, Stereology of arbitrary particles. A review of unbiased number and size estimators and the presentation of some new ones, in memory of William R. Thompson, *J Microsc*, **143**:3–45

Henle SJ, Wang G, Liang E, Wu M, Poo M, Henley JR. 2011, Asymmetric PI (3 , 4 , 5) P 3 and Akt Signaling Mediates Chemotaxis of Axonal Growth Cones, *J Neurosci*, **31**:7016–7027

Höke A, Redett R, Hameed H, Jari R, Zhou C, Li ZB, Griffin JW, Brushart TM. 2006, Schwann cells express motor and sensory phenotypes that regulate axon regeneration, *J Neurosci*, **26**:9646–9655.

Honig MG, Frase P, Camilli SJ. 1998, The spatial relationships among cutaneous, muscle sensory and motoneuron axons during development of the chick hindlimb, Development **125**:995–1004

Jesuraj NJ, Nguyen PK, Wood MD, Moore AM, Borschel GH, Mackinnon SE, Sakiyama-Elbert SE. 2012, Differential gene expression in motor and sensory Schwann cells in the rat femoral nerve, *J Neurosci Res*, **90**:96–104

Karchewski LA, Kim FA, Johnston J, McKnight RM, Verge VMK. 1999, Anatomical evidence supporting the potential for modulation by multiple neurotrophins in the majority of adult lumbar sensory neurons, *J Comp Neurol*, **413**:327–341

Lago N, Rodríguez FJ, Guzmán-Lenis MS, Jaramillo J, Navarro X. 2007, Effects of motor and sensory nerve transplants on amount and specificity of sciatic nerve regeneration, *J Neurosci Res*, **2812**:2800–2812

Li Y, Jia Y, Cui K, Li N, Zheng Z, Wang Y, Yuan X. 2005, Essential role of TRPC channels in the guidance of nerve growth cones by brain-derived neurotrophic factor, *Nature* **434**:1–5.

Lotfi P, Garde K, Chouhan A, Bengali E, Romero-Ortega M. 2011, Modality-specific axonal regeneration: toward selective regenerative neural interfaces, *Front Neuroeng*, **4**:11

Madison RD, Archibald SJ, Brushart TM. 1996, Reinnervation accuracy of the rat femoral nerve by motor and sensory neurons, *J Neurosci*, **16**:5698–5703.

Madison RD, Robinson G. Chadaram SR. 2007, The specificity of motor neurone regeneration (preferential reinnervation), *Acta Physiol*, **189**:201–6

Madorsky SJ, Swett JE, Crumley RL. 1998, Motor versus sensory neuron regeneration through collagen tubules, *Plast Reconstr Surg*, **102**:430–438

Martini R, Schachner M, Brushart TM. 1994, The L2/HNK-1 carbohydrate is preferentially expressed by previously motor axon-associated Schwann cells in reinnervated peripheral nerves, J Neurosci, **14**:7180–7191.

Martini R, Xin Y, Schmitz B, Schachner M. 1992, The L21HNK-1 Carbohydrate Epitope is Involved in the Preferential Outgrowth of Motor Neurons on Ventral Roots and Motor Nerves, *Eur J Neurosci*, **4**:628–639.

Meyer C, Stenberg L, González-Pérez F, Wrobel S, Ronchi G, Udina E, Suganuma S, Geuna S, Navarro X, Dahlin LB, Grothe C, Haastert-Talini K. 2016, Chitosan-film enhanced chitosan nerve guides for long-distance regeneration of peripheral nerves, *Biomaterials*, **76**:33–51

Ming G, Song H, Berninger B, Inagaki N, Tessier-lavigne M, Poo M. 1999, Phospholipase C- and Phosphoinositide 3-Kinase Mediate Cytoplasmic Signaling in Nerve Growth Cone Guidance University of California at San Diego, *Neuron*, **23**:139–148

Moore K, MacSween M, Shoichet M. 2006, Immobilized concentration gradients of neurotrophic factors guide neurite outgrowth of primary neurons in macroporous scaffolds, *Tissue Eng*, **12**:267–278

Navarro X, Verdú E, Butí M. 1994, Comparison of regenerative and reinnervating capabiblities of different fybers, *Exp Neurol*, **129**:217–224

Plantman S, Patarroyo M, Fried K, Domogatskaya A, Tryggvason K, Hammarberg H, Cullheim S. 2008, Integrin-laminin interactions controlling neurite outgrowth from adult DRG neurons in vitro, *Mol Cell Neurosci*; **39**:50–62.

Rende M, Granato A, Lo Monaco M, Zelano G, Tcesca A. 1991, Accuracy of reinnervation by peripheral nerve axons regenerating across a 10-mm gap within an impermeable chamber, *Exp Neurol*, **111**:332–339

Robinson GA, Madison RD. 2004, Motor neurons can preferentially reinnervate cutaneous pathways, *Exp Neurol*, **190**:407–413

Saito H, Nakao Y, Takayama S, Toyama Y, Asou H. 2005, Specific expression of an HNK-1 carbohydrate epitope and NCAM on femoral nerve Schwann cells in mice, *Neurosci Res*, **53**:314–322

Santos D, Giudetti G, Micera S, Navarro X, del Valle J. 2016a, Focal release of neurotrophic factors by biodegradable microspheres enhance motor and sensory axonal regeneration in vitro and in vivo, *Brain Res*, **1636**:93–106

Santos D, González-Pérez F, Giudetti G, Micera S, Udina E, Del Valle J, Navarro X. 2017a, Preferential enhancement of sensory and motor axon regeneration by combining extracellular matrix components with neurotrophic factors, *Int J Mol Sci*, **18.1**:65

Santos D, González-Pérez F, Navarro X, del Valle J. 2016b, Dose-Dependent Differential Effect of Neurotrophic Factors on In Vitro and In Vivo Regeneration of Motor and Sensory Neurons, *Neural Plast*, **2016**:13

Santos D, Wieringa P, Moroni L, Navarro X, Del Valle J. 2017b, PEOT/PBT Guides Enhance Nerve Regeneration in Long Gap Defects, *Adv Healthc Mater*, **6**:3

Schindelin J, Arganda-carreras I, Frise E, Kaynig V, Pietzsch T, Preibisch S, Rueden C, Saalfeld S, Schmid B, Tinevez J, White D.J, Hartenstein V, Tomancak P, Cardona A. 2013, Fiji - an Open Source platform for biological image analysis, *Nat Methods*, **9**:676–682.

Song H, Ming G, Poo M, Shiro M, Tomb J, White O, Kerlavage AR, Clayton RA, Sutton GG, Fleischmann RD, Ketchum KA, Klenk HP, Gill S, Dougherty BA, Nelson K, Quackenbush J, Zhou L, Kirkness EF, Peterson S, Loftus B, Richardson D, Dodson R, Khalak HG, Glodek A, Mckenney K, Fitzegerald LM, Lee N, Adams MD, Hickey EK, Berg DE, Gocayne JD, Utterback TR, Peterson JD, Kelley JM, Cotton MD, Weidman JM, Fujii C, Bowman C, Watthey L, Wallin E, Hayes WS, Borodovsky M, Karp PD, Smith HO, Fraser CM, Venter JC, Bergman MI. 1997, cAMP-induced switching in turning direction of nerve growth cones corrections, *Nature*, **389**:1211–1212

Takahashi Y, Maki Y, Yoshizu T, Tajima T. 1999, Both stump area and volume of distal sensory nerve segments influence the regeneration of sensory axons in rats, *Scand J Plast Reconstr Hand Surg*, **33**:177–180

Taylor MD, Holdeman AS, Weltmer SG, Ryals JM, Wright DE. 2005, Modulation of muscle spindle innervation by neurotrophin-3 following nerve injury, *Exp Neurol*, **191**:211–22

Tucker B, Mearow KM. 2008. Peripheral Sensory Axon Growth: From Receptor Binding to Cellular Signaling, *Can J Neurol Sci*, **35**:551–566

Turney SG, Bridgman PC. 2005, Laminin stimulates and guides axonal outgrowth via growth cone myosin II activity, *Nat Neurosci*, **8**:717–719

Uschold T, Robinson G, Madison RD. 2007, Motor neuron regeneration accuracy: balancing trophic influences between pathways and end-organs, *Exp Neurol*, **205**:250–6

Usoskin D, Furlan A, Islam S, Abdo H, Lönnerberg P, Lou D, Hjerling-Leffler J, Haeggström J, Kharchenko O, Kharchenko PV, Linnarsson S, Ernfors P. 2015, Unbiased classification of sensory neuron types by large-scale single-cell RNA sequencing, *Nat Neurosci*, **18**:145–153

Valero-Cabré A, Tsironis K, Skouras E, Navarro X, Neiss WF. 2004, Peripheral and spinal motor reorganization after nerve injury and repair, *J Neurotrauma*, **21**:95–108

Valero-Cabré A, Tsironis K, Skouras E, Perego G, Navarro X, Neiss WF. 2001, Superior muscle reinnervation after autologous nerve graft or poly-L-lactide-ε-caprolactone (PLC) tube implantation in comparison to silicone tube repair, *J Neurosci Res*, **63**:214–223

Verdú E, Labrador RO, Rodríguez FJ, Ceballos D, Forés J, Navarro X. 2002, Alignment of collagen and laminin-containing gels improve nerve regeneration within silicone tubes, *Restor Neurol Neurosci*, **20**:169–179

Vögelin E, Baker JM, Gates J, Dixit V, Constantinescu M, Jones NF. 2006, Effects of local continuous release of brain derived neurotrophic factor (BDNF) on peripheral nerve regeneration in a rat model, *Exp Neurol*, **199**:348–53

Webber C, Xu Y, Vanneste K, Martinez J, Verge V, Zochodne D. 2008, Guiding Adult Mammalian Sensory Axons During Regeneration, *J Neuropathol Exp Neurol*, 67:212–222

Yuan X, Jin M, Xu X, Song Y, Wu C, Poo M, Duan S. 2003, Signalling and crosstalk of Rho GTPases in mediating axon guidance, *Nat Cell Biol*, **5**:1–8

Zele T, Sketelj J, Bajrović FF. 2010, Efficacy of fluorescent tracers in retrograde labeling of cutaneous afferent neurons in the rat, *J Neurosci Methods*, **191**:208–14

Table 1. Average number of motor and sensory neurons that regenerated axons within each branch of the Y tube towards the distal inserts of T+S or P nerves.

	Control			Experimental		
	T+S	P	DL	T+S	P	DL
MN	654.6 ± 11.4	88.6 ± 36.6	139.6 ± 56.9	339.6 ± 60.8	497.2 ± 60.1	91.4 ± 31.47
SN	5173.6 ± 343	1846.6 ± 864.1	698.3 ± 117.3	4263.2 ± 1069.7	2609.2 ± 700.5	633 ± 166.64

7. Figure legends

Figure 1. Schematic drawing showing the design of the bicompartmental Y tube, and the contents of each branch in the control group (A) and in the experimental group (B). Micrograph of the implanted Y tube filled with a collagen gel at both distal branches of the tube (C). Micrograph of a regenerated nerve after the extraction of the tube prior to retrotracer application (D).

Figure 2. Plot of the pinprick score in the control and experimental groups during follow-up (A). Latency of withdrawal response to thermal algesimetry test in the lateral part of the paw during follow-up (B). Data expressed as mean ± SEM.

Figure 3. Histogram of the mean amplitude of the CMAP at 90 dpi in (A) Tibialis anterior (TA) muscle innervated by the peroneal nerve, (B) Gastrocnemius (GM) and (C) Plantar interossei (PL) muscles innervated by the tibial nerve. *$p<0.05$. Data expressed as mean ± SEM.

Figure 4. Representative micrographs of neurons retrolabeled with True Blue (TB) (A), Fluorogold (FG) (B) and double labeled (DL) (C). Representative micrographs of MNs retrolabeled in the spinal cord in control (D) and experimental conditions (F), and of SNs retrolabeled in DRG in control (E) and experimental conditions (G). In this case, FG was applied to the T+S distal nerve and TB to the P distal nerve. Histogram of the number of regenerated MNs in the spinal cord (H) and SNs in the DRG (I) in both control and experimental groups. Data expressed as mean ± SEM. ***$p<0.001$.

Figure 5. Morphometric analysis of regenerated SNs in the T+S nerves (A), P nerve (B) and in both branches (C) in the control (black bars) and experimental (white bars) groups. Histogram of regenerated small size (D), medium size (E) and large size sensory neurons (F) in the different branches of the Y tube in the two groups. Data expressed as mean ± SEM. *$p<0.05$.

Figure 1

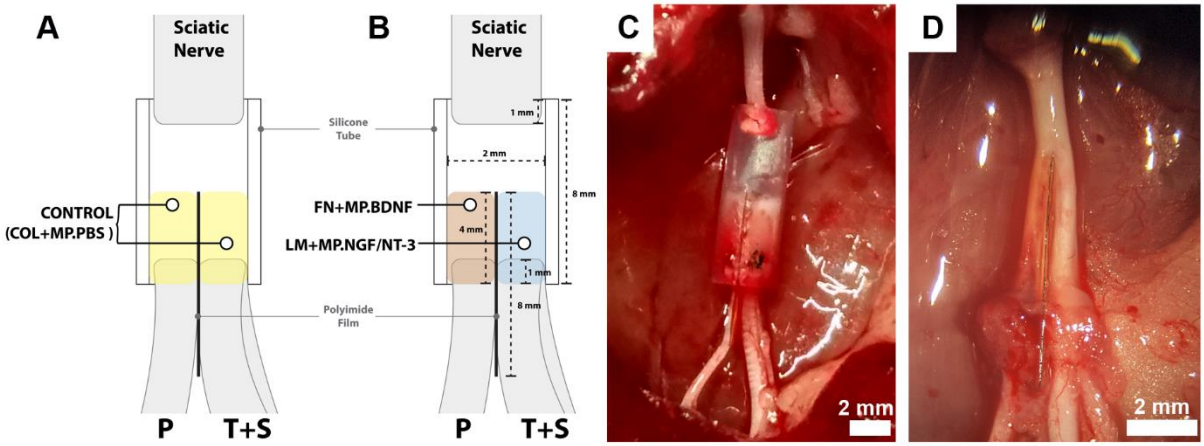
A
Sciatic Nerve
CONTROL (COL+MP.PBS)
P
T+S
B
Sciatic Nerve
Silicone Tube
1 mm
2 mm
8 mm
FN+MP.BDNF
4 mm
LM+MP.NGF/NT-3
1 mm
Polyimide Film
8 mm
P
T+S
C
2 mm
D
2 mm

Figure 2

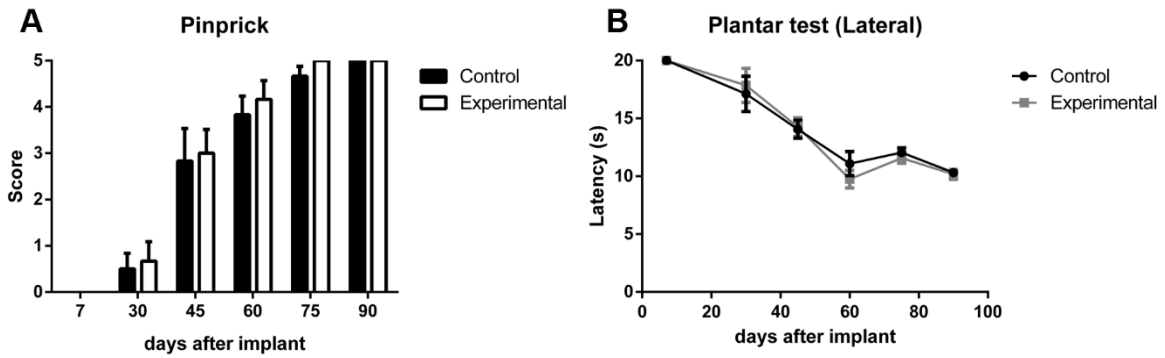
A
Pinprick
Score
0
1
2
3
4
5
7
30
45
60
75
90
days after implant
Control
Experimental
B
Plantar test (Lateral)
Latency (s)
0
5
10
15
20
0
20
40
60
80
100
days after implant
Control
Experimental

Figure 3

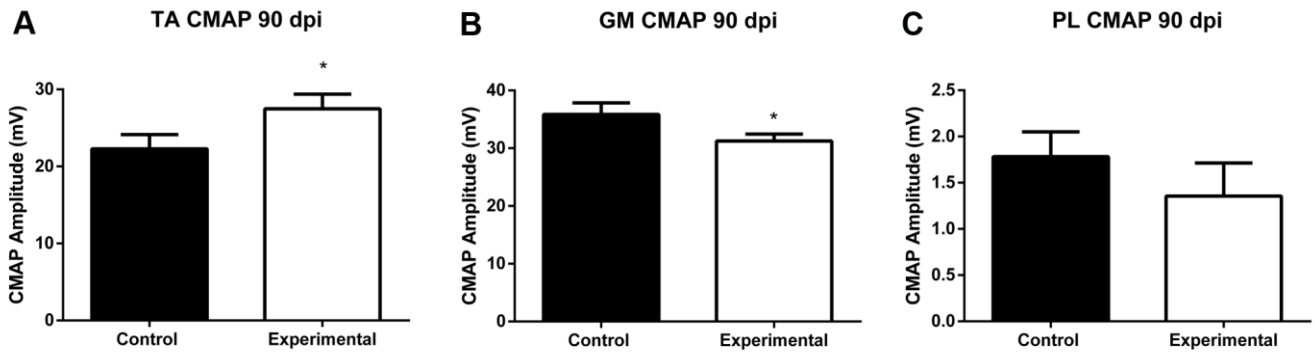
A
TA CMAP 90 dpi
CMAP Amplitude (mV)
30
20
10
0
*
Control
Experimental
B
GM CMAP 90 dpi
CMAP Amplitude (mV)
40
30
20
10
0
*
Control
Experimental
C
PL CMAP 90 dpi
CMAP Amplitude (mV)
2.5
2.0
1.5
1.0
0.5
0.0
Control
Experimental

Figure 4

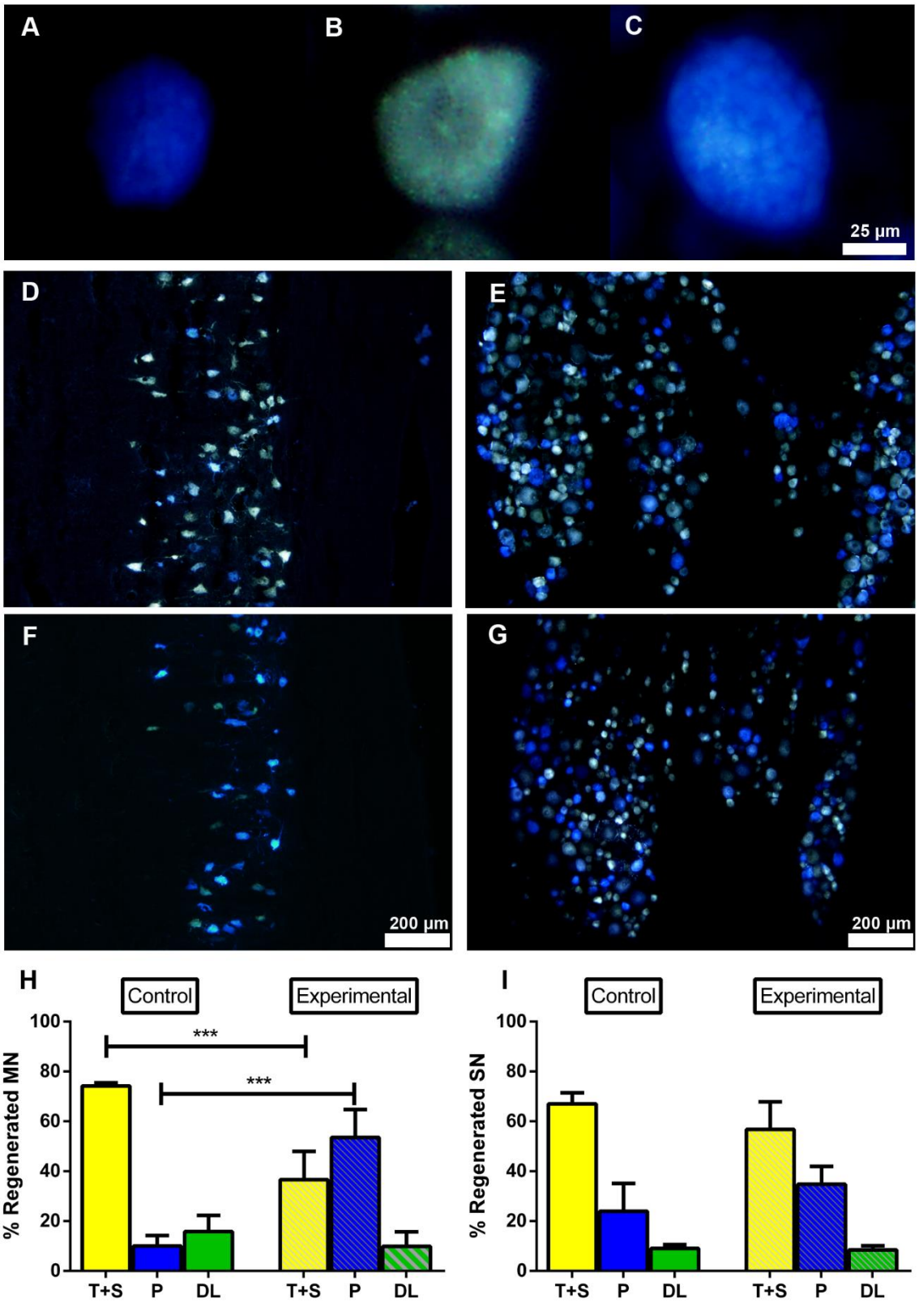
A
B
C
25 µm
D
E
F
200 µm
G
200 µm
H
Control
Experimental
***
***
% Regenerated MN
100
80
60
40
20
0
T+S
P
DL
T+S
P
DL
I
Control
Experimental
% Regenerated SN
100
80
60
40
20
0
T+S
P
DL
T+S
P
DL

Figure 5

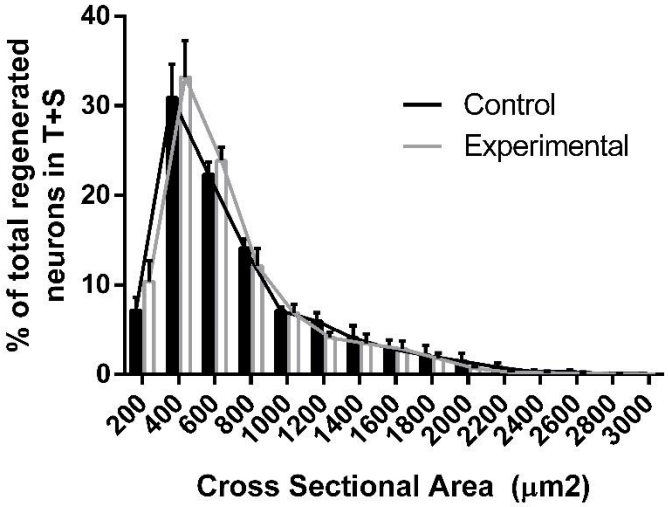
% of total regenerated neurons in T+S
Control
Experimental
Cross Sectional Area (μm2)

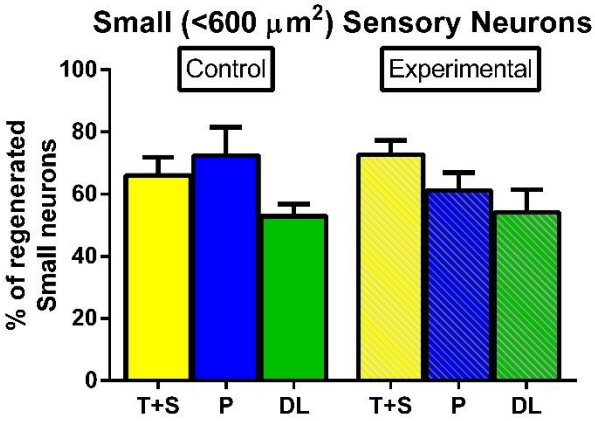
Small (<600 μm²) Sensory Neurons
Control
Experimental
% of regenerated Small neurons
T+S
P
DL

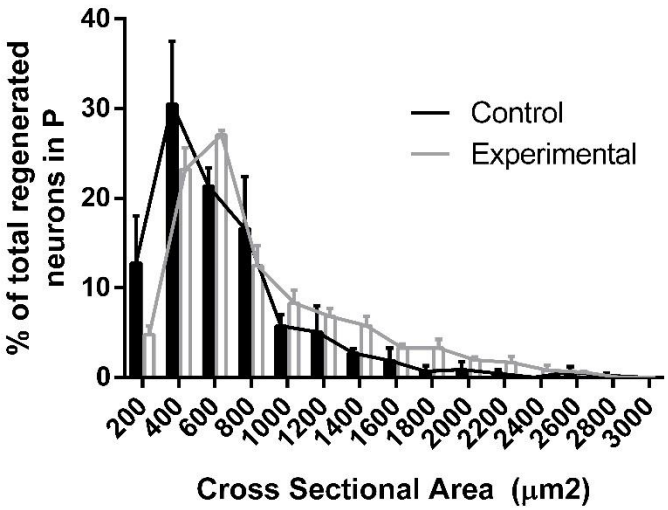
% of total regenerated neurons in P
Control
Experimental
Cross Sectional Area (μm2)

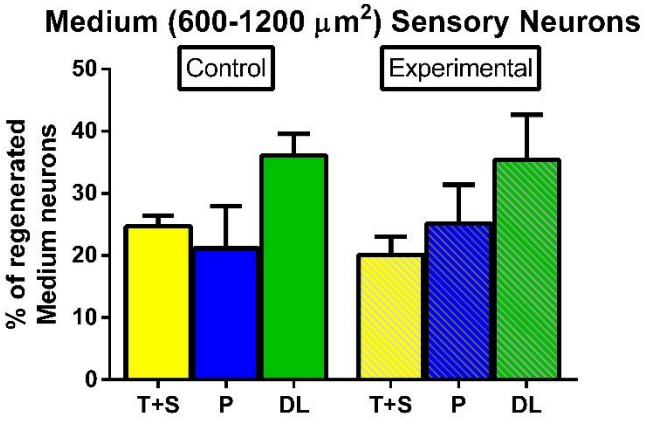
Medium (600-1200 μm²) Sensory Neurons
Control
Experimental
% of regenerated Medium neurons
T+S
P
DL

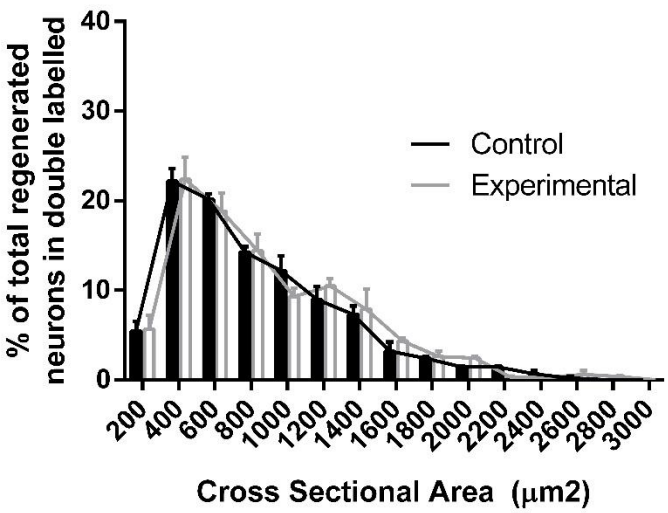
% of total regenerated neurons in double labelled
Control
Experimental
Cross Sectional Area (μm2)

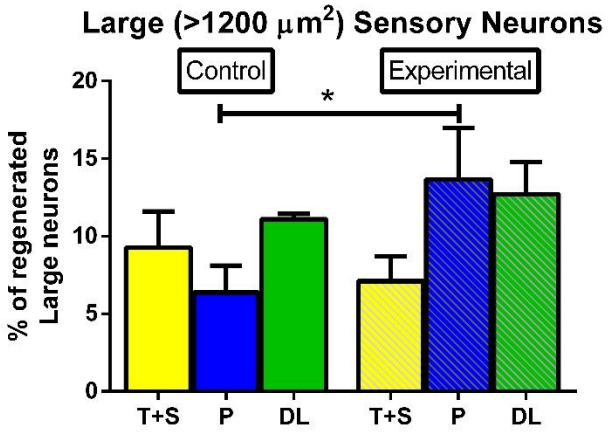
Large (>1200 μm²) Sensory Neurons
Control
Experimental
*
% of regenerated Large neurons
T+S
P
DL